Estimation and Comprehensive for Radiation and Neutron Shielding of Ni-base Superalloys: Inconel 600, 601, 617, 625, 625LCF, 686, 690 and 693

Sunantasak Ravangvong[1], Punsak Glumglomchit[2]*, Pitchaya Parnitvatthana[2], Nuttida Nimsean[2], Thantitcha Putthachatraksakul[2], Kittisak Sriwongsa[3,4], Chumphon Khobkham[5] and Wanna Wattana[6]

[1]Division of Science and Technology, Faculty of Science and Technology, Phetchaburi Rajabhat University, Phetchaburi, 76000, Thailand

[2]Huahinvitthayalai School, Hua-Hin, Prachuap Khiri Khan, 77110, Thailand

[3]Faculty of Education, Silpakorn University, Nakhon Pathom, 73000, Thailand

[4]The demonstration school of Silpakorn University, Nakhon Pathom, 73000, Thailand

[5]Faculty of Engineering, Thonburi University, Bangkok, 10160 Thailand

[6]Division of Chemistry, Faculty of Science and Technology, Phetchaburi Rajabhat University, Phetchaburi, 76000, Thailand

* Corresponding author. E-mail address: punsakk@gmail.com

Received: 15 May 2022; Revised: 3 August 2023; Accepted: 19 September 2023; Available online: 16 November 2023

Abstract

In this research, the radiation and neutron shielding properties of some Ni-base superalloys of Inconel 600, 601, 617, 625, 625LCF, 686, 690, and 693, were estimated. The radiation shielding effectiveness of the superalloys was estimated by determining the mass attenuation coefficient (μ_m), effective atomic number (Z_{eff}), effective electron density (N_{el}), half value layer (HVL) and mean free path (MFP) at photon energy ranging 1 keV-100 GeV using the WinXCom computer software program. Exposure and energy absorption buildup factors (EBF and EABF) were computed at energy levels ranging from 15 keV-15 MeV up to 40 mfp deep penetration. Neutron shielding was computed by partial density. The results showed that Inconel 686 superalloy was excellent radiation shielding. This study indicates that Inconel 686 superalloy can be developed as a radiation shielding medium. While Inconel 600 had the highest fast neutron removal cross sections (Σ_R value), meaning that Inconel 600 is better neutron shielding than the other Inconel samples.

Keywords: Ni-base superalloys, Gamma shielding, Neutron shielding

Introduction

The objective of this study of the properties of radiation shielding materials was to enhance the protection against dangerous radiation for workers and the environment. The materials for radiation shielding should consist of elements with high density and atomic number (Kavaz, Tekin, Kilic, & Susoy, 2020; Şakar, Özpolat, Alım, Sayyed, & Kurudirek, 2020; Issa, Rashad, Zakaly, Tekin, & Abouhaswa, 2020). Materials with amorphous structures, such as alloys, are widely used in many sectors because of their magnetic, mechanical, and chemical properties, making them of significant interest to researchers (Manjunatha, Seenappa, Chandrika, Sridhar, & Hanumantharayappa, 2018). Particularly, alloys containing heavy metals such as Ni, Cr, Fe, and Cu demonstrate increased radiation shielding efficiency (Sadawy & Shazly, 2019).

Ni-based superalloys (NBSA) are favored for use in several fields such as chemical manufacturing, aerospace and nuclear industries because of their superior overall performance in high-temperature environments (Sun, Chen, Li, & Ren, 2020). Inconel, a member of the NBSA series, is utilized in a variety of applications due to its high strength, weldability, formability, higher corrosion resistance, lack of post-weld heat treatment, and resistance to stress corrosion cracking (SCC) (Sriwongsa et al., 2022).

The effectiveness of Ni-base superalloys for radiation and neutron shielding of Inconel 600, 601, 617, 625, 625LCF, 686, 690 and 693 superalloys was explored in this study. Radiation shielding parameters: mass attenuation coefficient (μ_m), effective atomic number (Z_{eff}), effective electron density (N_{el}), half value layer (HVL) and mean free path (MFP) were estimated using the WinXCom software program at energies ranging from 1 keV to 100 GeV while buildup factors (BFs) were simulated using the G-P fitting method at energies ranging from 0.015 MeV to 15 MeV at deep penetration 1-40 mfp. Fast neutron removal cross sections (Σ_R) were calculated by the partial density method at energies in the range of 2-12 MeV. The results of this work can be applied to and developed for other materials.

Methods and Materials

Inconel samples

The radiation shielding properties of Inconel samples were simulated and explained using the WinXcom program (Alotaibi et al., 2021), which computed μ_m, Z_{eff}, N_{el}, MFP and HVL. BFs were calculated using the geometrical progression (G-P) fitting method (Levet & Özdemir, 2017; Sayyed & Elhouichet, 2017), and Σ_R was simulated using the partial density method (Abouhaswa, Rammah, Sayyed, & Tekin, 2019). All these values were identified from many previous articles (Singh & Badiger, 2014; Sriwongsa et al., 2020; ALMisned et al., 2021; Sriwongsa et al., 2022). The chemical compositions of the Inconel samples are exhibited in Table 1.

Table 1 Chemical composition for Inconel samples (wt%) (Alloy Handbook, 2022)

Inconel	**code**	Ni	C	Si	Mn	Cu	Fe	S	Nb	W
600	**S1**	72.000	0.150	0.500	1.000	0.500	6.000	0.015	–	–
		Co	Cr	Al	Ti	B	Mo	P	N	
		5.835	14.000	–	–	–	–	–	–	
Inconel	**code**	Ni	C	Si	Mn	Cu	Fe	S	Nb	W
601	**S2**	58.000	0.100	0.500	1.000	1.000	17.385	0.015	–	–
		Co	Cr	Al	Ti	B	Mo	P	N	
		–	21.000	1.000	–	–	–	–	–	
Inconel	**code**	Ni	C	Si	Mn	Cu	Fe	S	Nb	W
617	**S3**	55.029	0.050	1.000	1.000	0.500	3.000	0.015	–	–
		Co	Cr	Al	Ti	B	Mo	P	N	
		10.000	20.000	0.800	0.600	0.006	8.000	–	–	
Inconel	**code**	Ni	C	Si	Mn	Cu	Fe	S	Nb	W
625	**S4**	58.000	0.100	0.500	0.500	–	5.000	0.015	3.150	–
		Co	Cr	Al	Ti	B	Mo	P	N	
		3.920	20.000	0.400	0.400	–	8.000	0.015	–	
Inconel	**code**	Ni	C	Si	Mn	Cu	Fe	S	Nb	W
625LCF	**S5**	58.000	0.030	0.150	0.500	–	5.000	0.015	3.150	–
		Co	Cr	Al	Ti	B	Mo	P	N	
		4.320	20.000	0.400	0.400	–	8.000	0.015	0.020	
Inconel	**code**	Ni	C	Si	Mn	Cu	Fe	S	Nb	W
686	**S6**	61.080	0.010	0.080	0.750	–	1.000	0.020	–	3.000
		Co	Cr	Al	Ti	B	Mo	P	N	
		–	19.000	–	0.020	–	15.000	0.040	–	

Table 1 (Cont.)

Inconel	code									
		Ni	C	Si	Mn	Cu	Fe	S	Nb	W
		58.000	0.050	0.500	0.500	0.500	7.000	0.015	-	-
690	S7	Co	Cr	Al	Ti	B	Mo	P	N	
		6.435	27.000	-	-	-	-	-	-	
Inconel	**code**	Ni	C	Si	Mn	Cu	Fe	S	Nb	W
		64.335	0.150	0.500	1.000	0.500	2.500	0.015	0.500	-
693	S8	Co	Cr	Al	Ti	B	Mo	P	N	
		-	27.000	2.500	1.000	-	-	-	-	

Results and Discussion

1. Mass attenuation coefficient (μ_m), effective atomic number (Z_{eff}), effective electron density (N_{el}), half value layer (HVL) and mean free path (MFP)

The μ_m parameter for Inconel samples with energy is shown in Figure 1 which is a graph of variables for all Inconel samples. The μ_m values were maximum in the low energy ranges and rapidly declined in the intermediate energy ranges before increasing almost constant in the high energy range. The fundamental interactions of radiation with matters are the photoelectric effect (PE) as $\alpha\ E^{-1}$, the Compton scattering (CS) as $\alpha\text{-}E^{-1}$, and pair production (PP) as α ~~at~~ Log E. The discontinuities shown in the graphs at low energy ranges were due to the M-, L- and K-absorption edges of each element in the Inconel samples (Ravangvong et al., 2022) as exhibited in Table 2. Moreover, μ_m of sample S6 had the highest value because this sample contained the highest amount of tungsten (W).

Table 2 Absorption edges of each element in Inconel samples

Element	Absorption edges ($\times 10^{-3}$ MeV)								
	M5	**M4**	**M3**	**M2**	**M1**	**L3**	**L2**	**L1**	**K**
W	1.809	1.872	2.281	2.575	2.820	10.21	11.54	12.10	69.53
Mo						2.520	2.625	2.865	20.00
Nb						2.370	2.465	2.698	1.899
Ni								1.008	8.333
Cu								1.096	8.979
Si									1.839
Mn									6.539
Fe									7.112
S									2.472
Co									7.709
Cr									5.989
Al									1.560
Ti									4.966
P									2.145

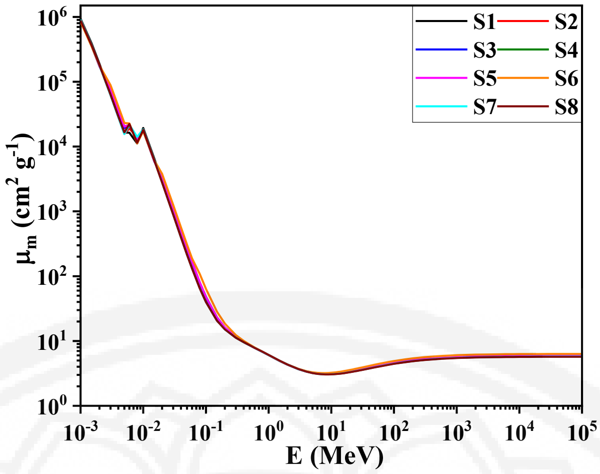

Figure 1 The μ_m of Inconel samples VS energy

The Z_{eff} and N_{el} of the Inconel samples are shown in Figures 2 and 3. As shown, both the Z_{eff} and N_{el} have the same characteristics and these parameters show a high value which indicates excellent radiation shielding. Both graphs show PE, CS, and PE varying with Z^{4-5}, Z, and Z^2, respectively (Singh et al., 2014; Singh, Kaur, Sharma, & Singh, 2018; Kaur, Sharma, & Singh, 2019; Boukhris et al., 2020). Due to the absorption edge of elements in the Inconel samples, both results indicate magnitudes. In addition, sample S6 had the highest Z_{eff} and N_{el} values indicating that this sample had superior radiation shielding.

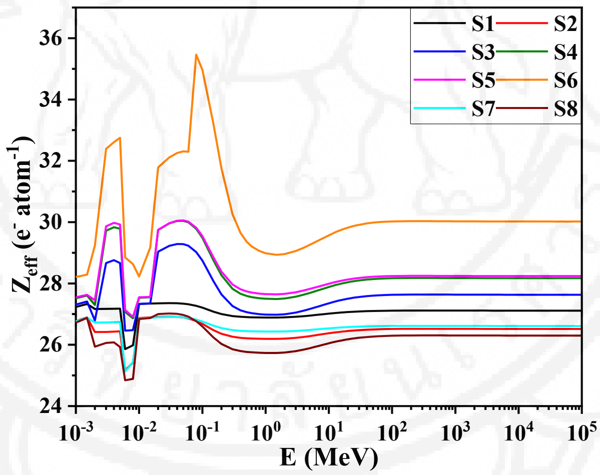

Figure 2 The Z_{eff} of Inconel samples VS energy

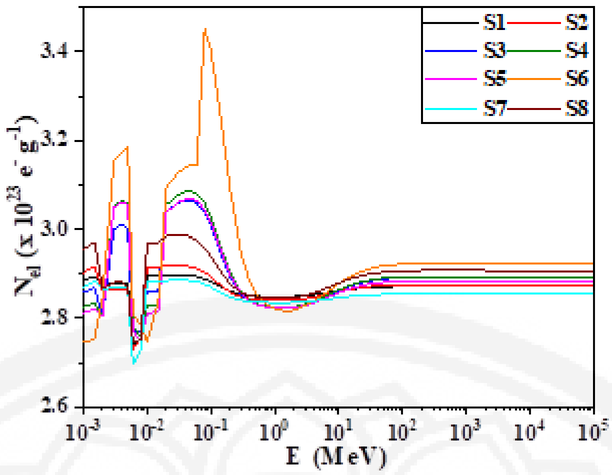

Figure 3 The N_{el} of Inconel samples VS energy

Normally, the radiation shielding medium should have low HVL and MFP values which increases the probability of radiation interaction with the shielding medium. Figures 4 and 5 show that sample S6 had low HVL and MFP values, which indicated that sample S6 is an excellent radiation-shielding medium (Issa et al., 2020).

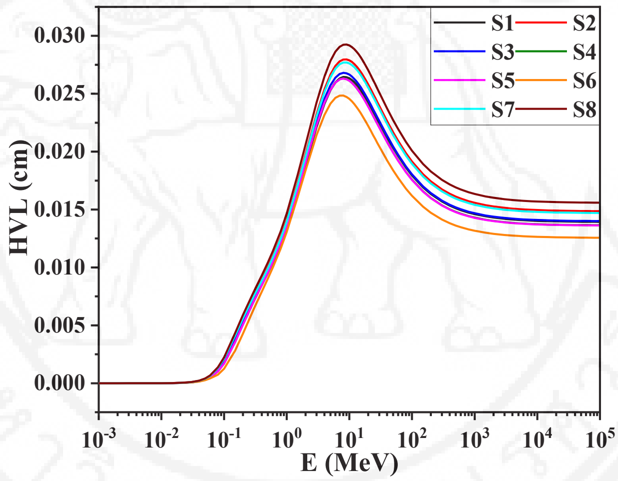

Figure 4 The HVL of Inconel samples VS energy

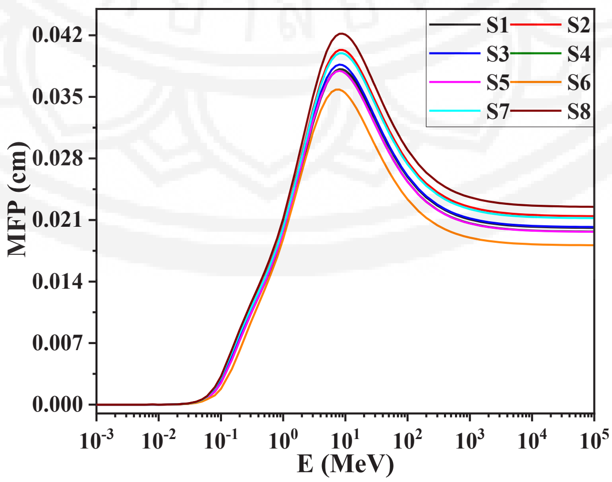

Figure 5 The MFP of Inconel samples VS energy

2. Buildup factors (BFs)

BFs are parameters used when discussing the absorption of radiation in material and air which are comprised of the energy absorption buildup factor (EABF) and the exposure buildup factor (EBF). Figure 7 (a-h) and 8 (a-h) show the simulated EABF and EBF values up to 40 mfp at an energy ranging of 0.015-15 MeV. Low energy ranges have low BFs because photons are absorbed since PE is the main mechanism of superiority, and the magnitudes of these ranges are due to the absorption edge (K-edge) of each element, as previously explained. At intermediate energy ranges, BFs values increased because of the photons' multiple scattering and the accumulation of photons, with CS as the main process. At high energy ranges, the BFs values are low due to PP being the main process by which photons absorb energy (Singh, Badiger, Chanthima, & Kaewkhao, 2014; Issa, Sayyed, Zaid, & Matori, 2017). Sample S6 showed the lowest value and the highest value of Z_{eq} as shown in Figure 6. Figures 9 and 10 illustrate the increase in BFs values with deep penetration for all Inconel samples, at specific energy levels (0.015, 0.15, 1.5, and 15 MeV). EABF and EBF values are essentially consistent at 0.015 MeV (Figure 9 and 10a). EABF and EBF values are independent of chemical composition at energies of 0.15 and 1.5 MeV (Figure 9 and 10b, c), and subsequently EABF and EBF values according to Z_{eq} at energies of 15 MeV (Figure 9 and 10d). These results indicated that S6 is a superior radiation-shielding material.

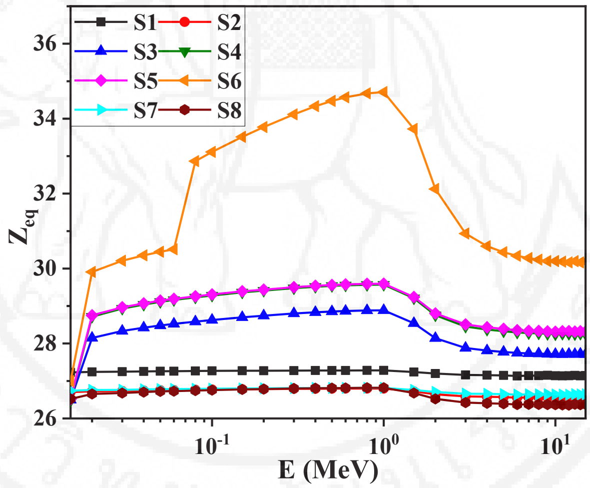

Figure 6 The Z_{eq} of Inconel samples VS energy

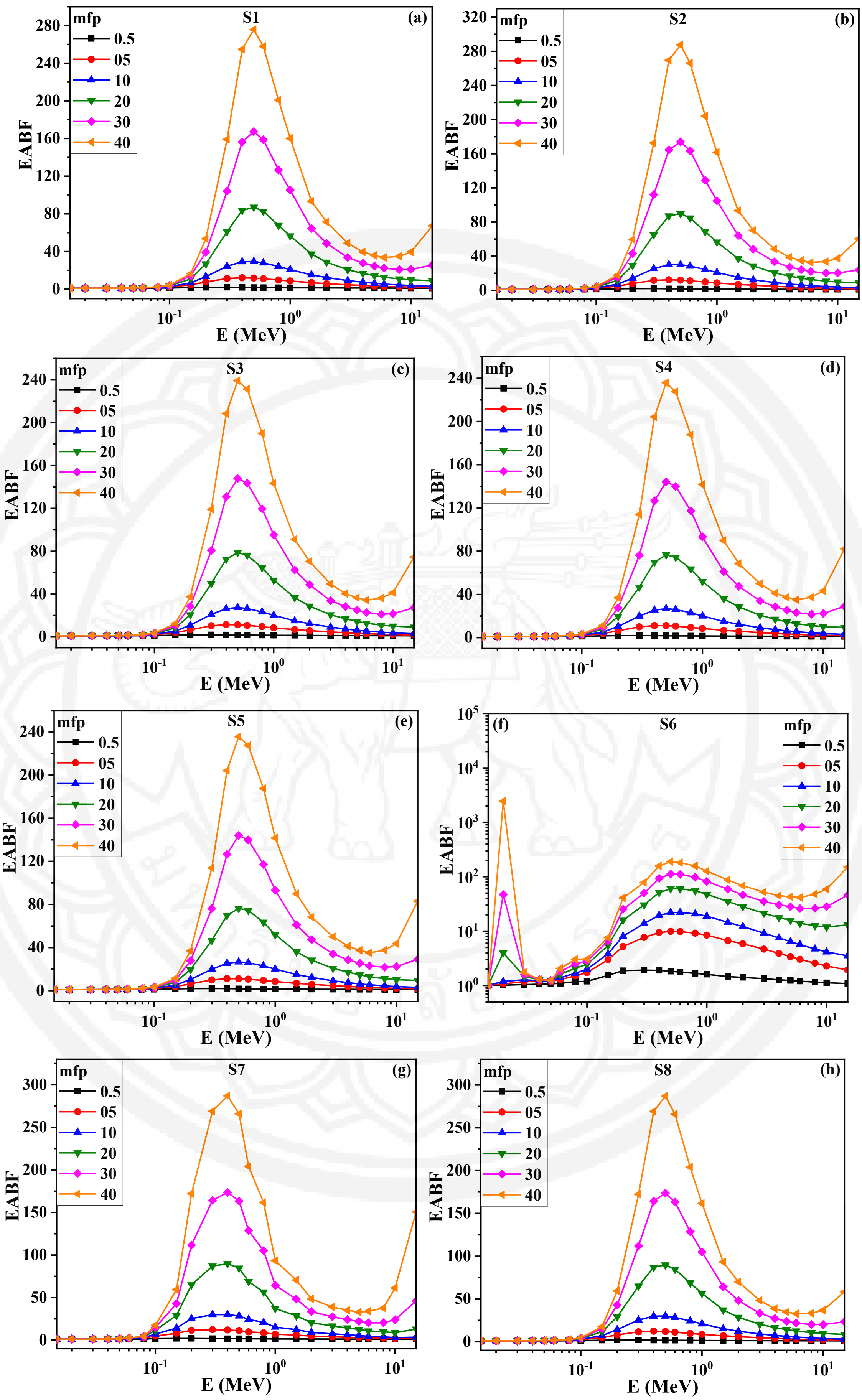

Figure 7 (a-h). EABF of samples VS energy at 1-40 mfp

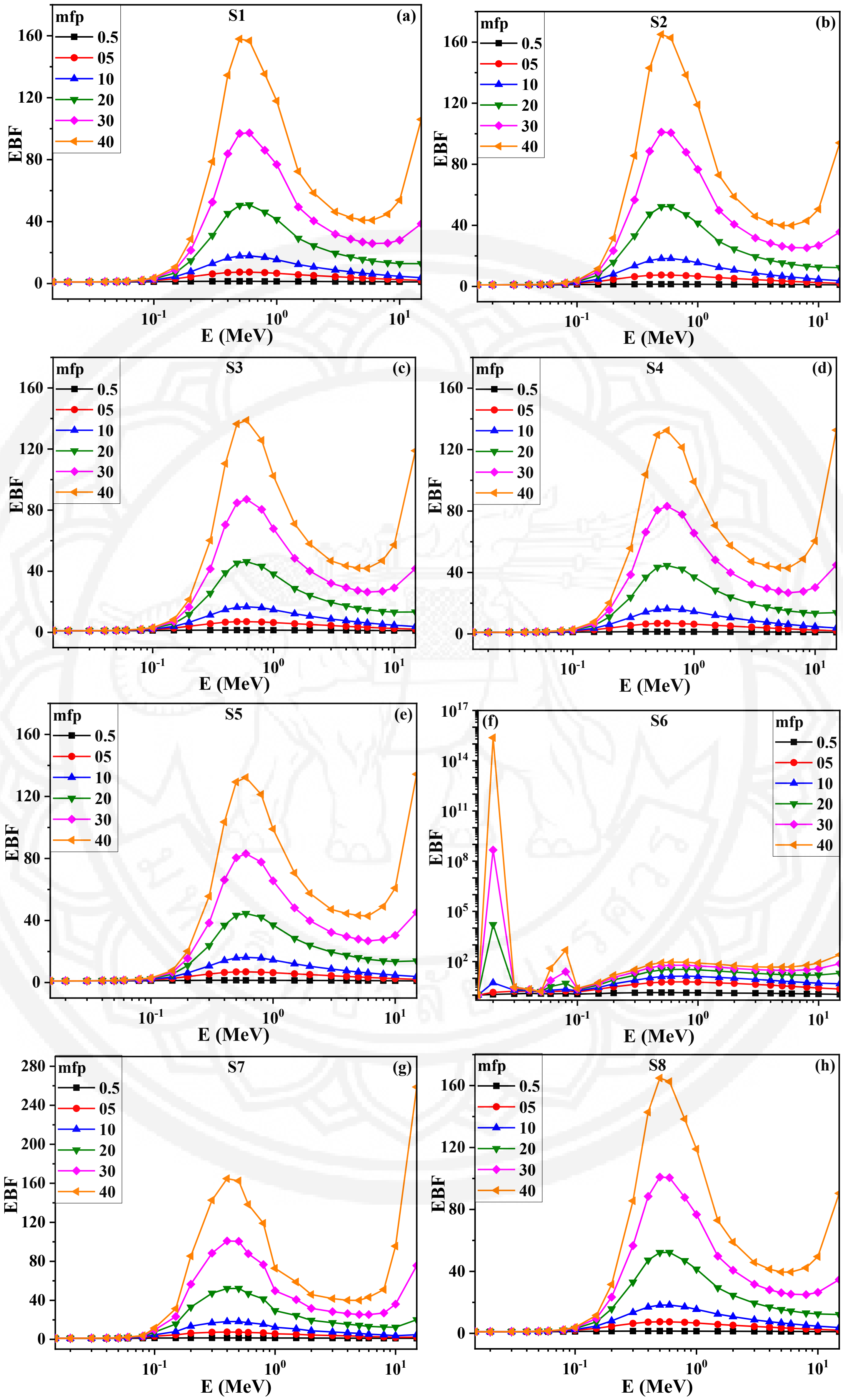

Figure 8 (a-h). EBF of samples VS energy at 1-40 mfp

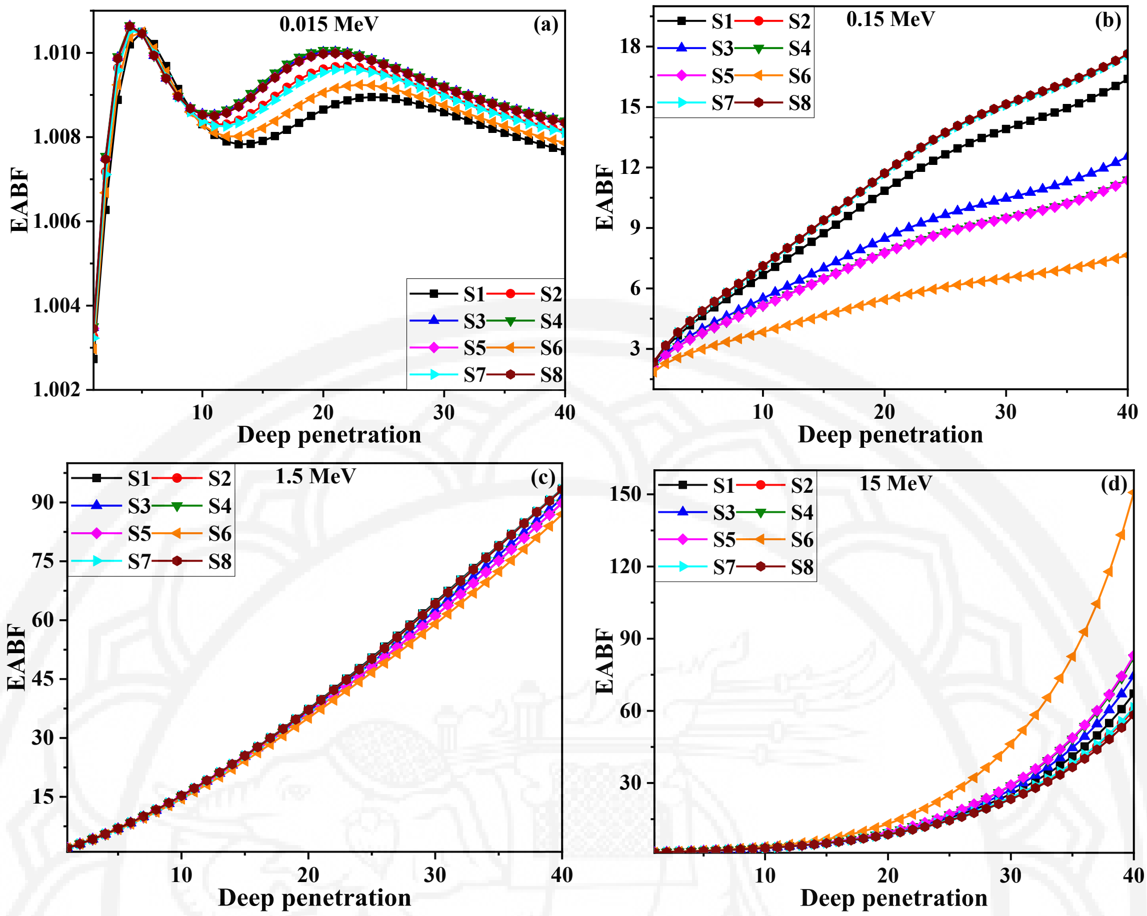

Figure 9 (a-d). EABF for Inconel samples up to 40 mfp at specific energies

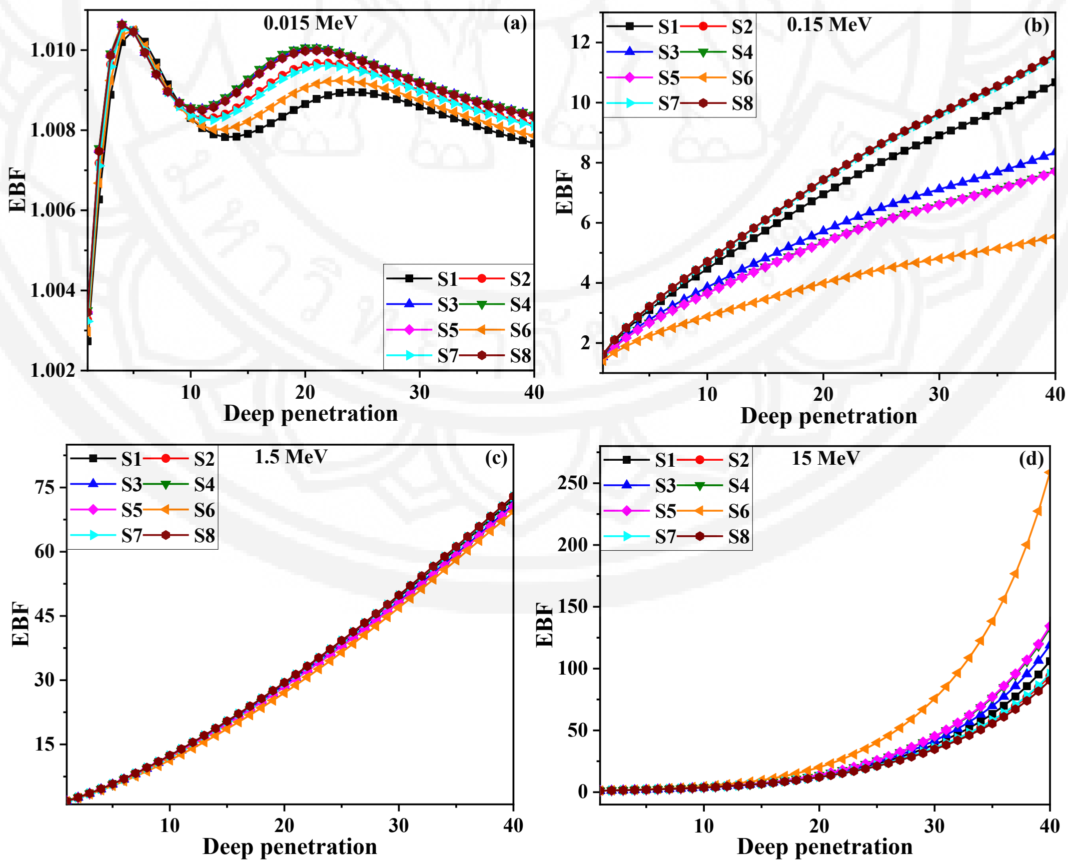

Figure 10 (a-d) EBF for Inconel samples up to 40 mfp at specific energies

3. Fast neutron removal cross sections (Σ_R)

Figure 11 shows Σ_R for Inconel samples. It is generally known that Σ_R decreases when the content of high-Z elements increases. The Inconel sample S1 has the highest Σ_R value, indicating that it has a higher neutron shielding than other Inconel samples.

This work estimated the radiation and neutron shielding properties of some Ni-base superalloys of Inconel 600, 601, 617, 625, 625LCF, 686, 690 and 693. The μ_m, Z_{eff}, N_{el}, HVL and MFP were determined at energy levels from 1 keV to 100 GeV. BFs were simulated at energy levels from 0.015 to 15MeV at deep penetration of 1-40 mfp. The Σ_R was determined by the partial density method. The results showed that PE, CS and PP are the main processes at low, intermediate and high energy ranges, respectively. In addition, the μ_m, Z_{eff}, N_{el}, HVL and MFP values are dependent on the energy level and Inconel 686, sample S6, showed the highest value while the lowest HVL and MFP values also included BFs. These results indicate that Inconel 686 is the best radiation shielding medium. The determination of Σ_R of Inconel samples at an energy ranging from 2 to 12 MeV, showed that Σ_R of Inconel 600 has the highest value. It means that Inconel 600 is better neutron shielding than the other Inconel samples. And this work is a simulation that can be developed with other materials.

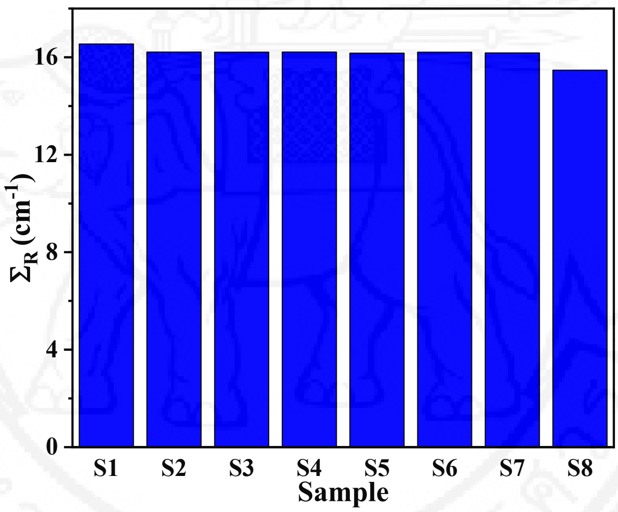

Figure 11 Σ_R of Inconel samples

Conclusion and Suggestions

This work estimated the radiation and neutron shielding properties of some Ni-based superalloys of Inconel 600, 601, 617, 625, 625LCF, 686, 690, and 693. The μ_m, Z_{eff}, N_{el}, HVL, and MFP were determined at different energy from 1 keV to 100 GeV. As well, BFs were simulated at energy from 0.015 to 15MeV at deep penetration 1-40 mfp. The Σ_R was determined by the partial density method. The results showed that PE is the main process at low energy ranges, CS at intermediate energy ranges, and PP is the main process at high energy ranges. In addition, the μ_m, Z_{eff}, N_{el}, HVL and MFP values are dependent on energy levels and Inconel 686, sample S6 in our study, showed the highest value while the lowest HVL and MFP values also included BFs. These results indicated that Inconel 686 is the best radiation shielding medium. The determination of Σ_R of Inconel samples at an energy ranging from 2 to 12 MeV, it's exhibited that Σ_R of Inconel 600 has the highest value. It means that Inconel 600 is better neutron shielding than the other Inconel samples.

Acknowledgements

The researchers would like to thank Silpakorn University, Thailand for supporting this article.

References

Abouhaswa, A. S., Rammah, Y. S., Sayyed, A. I., & Tekin, H. O. (2019). Synthesis, structure, optical and gamma radiation shielding properties of B_2O_3-PbO_2-Bi_2O_3 glasses. *Composites Part B, 172*, 218-225.

ALMisned, G., Tekin, H. O., Kavaz, E., Bilal, G., Issa, S. A. M., Zakaly, H. M. H., & Ene, A. (2021). Gamma, Fast Neutron, Proton, and Alpha Shielding Properties of Borate Glasses: A Closer Look on Lead (II) Oxide and Bismuth (III) Oxide Reinforcement. *Applied Sciences, 11*, 6837.

Alloy Handbook. (2022). *Product handbook of High-Performance Nickel Alloys.* Retrieved from https://www.specialmetals.com/documents/nickel-alloy-handbook.pdf

Alotaibi, B. M., Alotiby, M., Kumar, A., Mahmoud, K. A., Sayyed, M. I., Al-Yousef, H. A., Al-Hadeethi, Y. (2021). Gamma-ray shielding, physical, and structural characteristics of TeO_2-CdO-PbO-B_2O_3 glasses. *Optical Materials, 119*, 111333.

Boukhris, I., Al-Buriahi, M. S., Akyildirim, H., Alalawi, A., Kebaili, I., & Sayyed, M. I. (2020). Chalcogenide glass ceramics for radiation shielding applications. *Ceramics International, 46*(11), 19385-19392.

Issa, S. A. M., Rashad, M., Zakaly, H. M. H., Tekin, H. O., & Abouhaswa, A. S. (2020). Nb_2O_5-Li_2O-Bi_2O_3-B_2O_3 novel glassy system: evaluation of optical, mechanical, and gamma shielding parameters. *Journal of Materials Science: Materials in Electronics, 31*(24), 1-18.

Issa, S. A. M., Sayyed, M. I., Zaid, M. H. M., & Matori, K. A. (2017). A comprehensive study on gamma rays and fast neutron sensing properties of GAGOC and CMO scintillators for shielding radiation applications. *Journal of Spectroscopy, 2017*, 1.

Kaur, T., Sharma, J., & Singh, T. (2019). Review on the scope of metallic alloys in gamma rays shield designing. *Progress in Nuclear Energy, 113*, 95-113.

Kavaz, E., Tekin, H. O., Kilic, G., & Susoy, G. (2020). Newly developed Zinc-Tellurite glass system: An experimental investigation on the impact of Ta_2O_5 on nuclear radiation shielding ability. *Journal of Non-Crystalline Solids, 544*, 120169.

Levet, A., & Özdemir, Y. (2017). Determination of effective atomic numbers, effective electrons numbers, total atomic cross-sections and buildup factor of some compounds for different radiation sources. *Radiation Physics and Chemistry, 130*, 171-176.

Manjunatha, H. C., Seenappa, L., Chandrika, B. M., Sridhar, K. N., & Hanumantharayappa, C. (2018). Gamma, X-ray and neutron shielding parameters for the Al-based glassy alloys. *Applied Radiation and Isotopes, 139*, 187-194.

Ravangvong, S., Nisspa, W., Glumglomchit, P., Amornsophon, P., Kanuenghet, R., Pakdeepensuk P., ... Kaewkhao, J. (2022). Effects of WO_3 on Radiation Shielding Properties of WO_3-TeO_2 Binary Tellurite Glass System. *Integrated Ferroelectrics, 222*, 125-135.

Sadawy, M. M., & El Shazly, R. M. (2019). Nuclear radiation shielding effectiveness and corrosion behavior of some steel alloys for nuclear reactor systems. *Defence Technology, 15*(4), 621-628.

Şakar, E., Özpolat, Ö. F., Alım, B., Sayyed, M. I., & Kurudirek, M. (2020). Phy-X / PSD: Development of a user friendly online software for calculation of parameters relevant to radiation shielding and dosimetry. *Radiation Physics and Chemistry, 166*, 108496.

Sayyed, M. I., & Elhouichet, H. (2017). Variation of energy absorption and exposure buildup factors with incident photon energy and penetration depth for boro-tellurite (B_2O_3-TeO_2) glasses. *Radiation Physics and Chemistry, 130*, 335-342.

Singh, V. P., & Badiger, N. M. (2014). Gamma ray and neutron shielding properties of some alloy materials. *Annals of Nuclear Energy, 64*, 301-310.

Singh, T., Kaur, A., Sharma, J., & Singh, P. S. (2018). Gamma rays' shielding parameters for some Pb-Cu binary alloys. *Engineering Science and Technology, an International Journal, 21*(5), 1078-1085.

Singh, V. P., Badiger, N. M., Chanthima, N., & Kaewkhao, J. (2014). Evaluation of gamma-ray exposure buildup factors and neutron shielding for bismuth borosilicate glasses. *Radiation Physics and Chemistry, 98*, 14-21.

Sriwongsa, K., Glumglomchit, P., Sualuang, B., Arunoros, P., Pansuay, M., Ravangvong, S., & Khobkham, C. (2022). Shielding of uncharged and charged radiation of PbO- B_2O_3- SiO_2- Na_2O glass system. *Naresuan University Journal: Science and Technology, 1*(30), 109-119.

Sriwongsa, K., Laopoonphol, N., Ariyalerdchai, S., Glumglomchit, P., Pungpang, N., Ravangvong, S., & Khobkham, C. (2020). The Comparative Study of Photon Shielding Properties of MoNbCrVTi and MoNbCrZrTi Alloy Materials. *Suranaree Journal of Science and Technology, 27*(4), 010023, 1-6.

Sriwongsa, K., Sirimongkolchaikul, J., Sukrasorn, C., Bussaparoek, T., Kanunghet, S., Phansuea, T., … Kaewkhao, J. (2022). Radiation and Fast Neutron Shielding Properties of Nickel- Based Superalloys: Inconel 600, 718 and 725 Superalloys. *Integrated Ferroelectrics, 224*, 120-133.

Sun, Y., Chen, L., Li, L., & Ren, X. (2020). High-temperature oxidation behavior and mechanism of Inconel 625 superalloy fabricated by selective laser melting. *Optics and Laser Technology, 132*, 106509.